mathematics

MDPI

Article

Stability Condition of the Second-Order SSP-IMEX-RK Method for the Cahn–Hilliard Equation

Hyun Geun Lee

Department of Mathematics, Kwangwoon University, Seoul 01897, Korea; leeh1@kw.ac.kr

Received: 7 November 2019; Accepted: 17 December 2019; Published: 19 December 2019

check for updates

Abstract: Strong-stability-preserving (SSP) implicit–explicit (IMEX) Runge–Kutta (RK) methods for the Cahn–Hilliard (CH) equation with a polynomial double-well free energy density were presented in a previous work, specifically H. Song's "Energy SSP-IMEX Runge–Kutta Methods for the Cahn–Hilliard Equation" (2016). A linear convex splitting of the energy for the CH equation with an extra stabilizing term was used and the IMEX technique was combined with the SSP methods. And unconditional strong energy stability was proved only for the first-order methods. Here, we use a nonlinear convex splitting of the energy to remove the condition for the convexity of split energies and give a stability condition for the coefficients of the second-order method to preserve the discrete energy dissipation law. Along with a rigorous proof, numerical experiments are presented to demonstrate the accuracy and unconditional strong energy stability of the second-order method.

Keywords: Cahn–Hilliard equation; energy stability; implicit–explicit methods; Runge–Kutta methods

---

1. Introduction

In this paper, we consider the Cahn–Hilliard (CH) equation [1]:

$$\frac{\partial \phi}{\partial t} = M\Delta\left(F'(\phi) - \epsilon^2\Delta\phi\right), \tag{1}$$

where ϕ is the order parameter, $M > 0$ is a mobility, $F(\phi) = \frac{1}{4}(\phi^2 - 1)^2$ is a polynomial double-well free energy density, and $\epsilon > 0$ is the gradient energy coefficient. We assume that ϕ and $\nabla\phi$ are periodic along the normal to the boundary of a domain $\Omega \subset \mathbb{R}^d$ $(d = 1, 2, 3)$. The CH equation has been applied to a wide range of problems [2] and is an H^{-1}-gradient flow of the following free energy functional:

$$\mathcal{E}(\phi) := \int_\Omega \left(F(\phi) + \frac{\epsilon^2}{2}|\nabla\phi|^2\right) d\mathbf{x}, \tag{2}$$

i.e., $\frac{\partial\phi}{\partial t} = M\Delta\frac{\delta\mathcal{E}}{\delta\phi}$, where $\frac{\delta}{\delta\phi}$ denotes the variational derivative. Thus, $\mathcal{E}(\phi)$ is nonincreasing in time.

The interesting coarsening process of large systems usually occurs on a very long time scale. Therefore, energy stable schemes with high-order time accuracy are highly desirable to perform long time simulations for the coarsening process and there are various related works. Gomez and Hughes introduced a second-order semi-implicit method based on the Crank–Nicolson method [3]. In [4], Guan et al. presented a second-order convex splitting scheme by combining the convex splitting idea [5,6] and the secant method [7]. Yang developed first- and second-order schemes based on the invariant energy quadratization idea [8]. In [9], Shin et al. proposed high-order (up to third-order) convex splitting schemes by combining the convex splitting idea and the specially designed implicit–explicit (IMEX) Runge–Kutta (RK) method. Shen et al. [10] presented second-order backward differentiation and Crank–Nicolson formulas based on the scalar auxiliary variable approach.

In [11–13], Gong et al. proposed high-order (up to sixth-order) schemes by combining the energy quadratization technique and a specific class of RK methods. Recently, strong-stability-preserving (SSP) IMEX-RK methods for the CH equation were presented [14]. The main idea of the methods was to use a linear convex splitting of $\mathcal{E}(\phi)$ with an extra stabilizing term (convex and concave parts of $\mathcal{E}(\phi)$ are treated implicitly and explicitly, respectively) and combine the IMEX technique [15,16] with the SSP methods [17–19]. In [14], unconditional strong energy stability (the energy is bounded by its value at the previous time step) was proved only for the first-order time-accurate methods.

In our work, we concentrate mainly on energy stability of the second-order time-accurate (three-stage) SSP-IMEX-RK method for the CH equation. The main issue, which is different from that in [14], consists of two aspects. First, we use a nonlinear convex splitting of $\mathcal{E}(\phi)$ to remove the condition for the convexity of split energies. Second, we give a stability condition for the coefficients of the second-order method to preserve the discrete energy dissipation law.

This paper is organized as follows. In Section 2, we present the second-order method with the nonlinear convex splitting and prove the method with the stability condition is unconditionally strongly energy stable. In Section 3, we present numerical examples showing the accuracy and energy stability of the method. Finally, conclusions are drawn in Section 4.

2. Second-Order SSP-IMEX-RK Method and Its Stability Condition

In order to present the second-order SSP-IMEX-RK method for the CH equation, we split $\mathcal{E}(\phi)$ into convex and concave parts [5,6]:

$$\mathcal{E}(\phi) = \mathcal{E}_c(\phi) - \mathcal{E}_e(\phi) = \int_\Omega \left(\frac{\phi^4}{4} + \frac{1}{4} + \frac{\epsilon^2}{2}|\nabla\phi|^2 \right) d\mathbf{x} - \int_\Omega \frac{\phi^2}{2}\, d\mathbf{x}. \tag{3}$$

Then, we have the following lemma.

Lemma 1. *The convexity of $\mathcal{E}_c(\phi)$ and $\mathcal{E}_e(\phi)$ yields the following inequality:*

$$\mathcal{E}(\phi) - \mathcal{E}(\psi) \le \left(\frac{\delta\mathcal{E}_c(\phi)}{\delta\phi} - \frac{\delta\mathcal{E}_e(\psi)}{\delta\phi}, \phi - \psi \right). \tag{4}$$

Proof. We refer to [20]. □

Combining the nonlinear convex splitting (3) with the second-order (three-stage) SSP-IMEX-RK method, we obtain the following scheme:

$$\begin{aligned}
\phi^{(1)} &= \phi^n + M\Delta t\, \Delta \left(\frac{\delta\mathcal{E}_c(\phi^{(1)})}{\delta\phi} - \frac{\delta\mathcal{E}_e(\phi^n)}{\delta\phi} \right), \\
\phi^{(2)} &= \alpha_{10}\phi^n + \alpha_{11}\phi^{(1)} + \beta_1 M\Delta t\, \Delta \left(\frac{\delta\mathcal{E}_c(\phi^{(2)})}{\delta\phi} - \frac{\delta\mathcal{E}_e(\phi^{(1)})}{\delta\phi} \right), \\
\phi^{n+1} &= \alpha_{20}\phi^n + \alpha_{21}\phi^{(1)} + \alpha_{22}\phi^{(2)} + \beta_2 M\Delta t\, \Delta \left(\frac{\delta\mathcal{E}_c(\phi^{n+1})}{\delta\phi} - \frac{\delta\mathcal{E}_e(\phi^{(2)})}{\delta\phi} \right),
\end{aligned} \tag{5}$$

where the coefficients $\alpha_{10}, \alpha_{11}, \alpha_{20}, \alpha_{21}, \alpha_{22}, \beta_1, \beta_2$ satisfy the second-order conditions:

$$\begin{cases}
\alpha_{10} + \alpha_{11} = 1, \\
\alpha_{20} + \alpha_{21} + \alpha_{22} = 1, \\
\alpha_{21} + \alpha_{22}\alpha_{11} + \alpha_{22}\beta_1 + \beta_2 = 1, \\
\alpha_{21} + \alpha_{22}\alpha_{11} + \alpha_{22}\alpha_{11}\beta_1 + \alpha_{22}\beta_1^2 + \alpha_{21}\beta_2 + \alpha_{22}\alpha_{11}\beta_2 + \alpha_{22}\beta_1\beta_2 + \beta_2^2 = \frac{1}{2}, \\
\alpha_{22}\beta_1 + \alpha_{11}\beta_2 + \beta_1\beta_2 = \frac{1}{2}.
\end{cases}$$

The above system is under-determined and does not have a unique solution. Examples of the coefficients are listed in (7)–(10).

Definition 1. *(Stability Condition). Define a matrix* $\mathbf{M}$ *given by*

$$\mathbf{M} = \begin{pmatrix} \beta_2 & 0 & 0 \\ (\alpha_{22}-1)\beta_1 & \beta_1 & 0 \\ \alpha_{11}(\alpha_{22}-1)+\alpha_{21} & -\alpha_{10} & 1 \end{pmatrix}.$$

The stability condition is defined as

$$\mathbf{M} \textit{ is positive semi-definite.} \tag{6}$$

Next, we show that the scheme (5) with their coefficients satisfying the stability condition is unconditionally strongly energy stable.

Theorem 1. *The scheme* (5) *with their coefficients satisfying the stability condition* (6) *is unconditionally strongly energy stable, i.e., it satisfies*

$$\mathcal{E}(\phi^{n+1}) \leq \mathcal{E}(\phi^n)$$

for any time step $\Delta t > 0$.

Proof. Using Lemma 1, we have

$$\begin{aligned}
&\mathcal{E}(\phi^{n+1}) - \mathcal{E}(\phi^n) \\
&= \Big(\mathcal{E}(\phi^{n+1}) - \mathcal{E}(\phi^{(2)})\Big) + \Big(\mathcal{E}(\phi^{(2)}) - \mathcal{E}(\phi^{(1)})\Big) + \Big(\mathcal{E}(\phi^{(1)}) - \mathcal{E}(\phi^n)\Big) \\
&\leq \Big(\mu^{n+1}, \phi^{n+1} - \phi^{(2)}\Big) + \Big(\mu^{(2)}, \phi^{(2)} - \phi^{(1)}\Big) + \Big(\mu^{(1)}, \phi^{(1)} - \phi^n\Big),
\end{aligned}$$

where $\mu^{n+1} = \frac{\delta\mathcal{E}_c(\phi^{n+1})}{\delta\phi} - \frac{\delta\mathcal{E}_e(\phi^{(2)})}{\delta\phi}$, $\mu^{(2)} = \frac{\delta\mathcal{E}_c(\phi^{(2)})}{\delta\phi} - \frac{\delta\mathcal{E}_e(\phi^{(1)})}{\delta\phi}$, and $\mu^{(1)} = \frac{\delta\mathcal{E}_c(\phi^{(1)})}{\delta\phi} - \frac{\delta\mathcal{E}_e(\phi^{n})}{\delta\phi}$. The second-step of (5) can be rewritten as follows:

$$\phi^{(2)} - \phi^{(1)} = \alpha_{11}(\phi^{(1)} - \phi^n) + M\Delta t\,\Delta(\beta_1\mu^{(2)} - \mu^{(1)}) = M\Delta t\,\Delta(\beta_1\mu^{(2)} - \alpha_{10}\mu^{(1)}).$$

And the third-step of (5) is

$$\begin{aligned}
\phi^{n+1} - \phi^{(2)} &= \alpha_{22}(\phi^{(2)} - \phi^{(1)}) + (-\alpha_{11} + \alpha_{21} + \alpha_{22})(\phi^{(1)} - \phi^n) + M\Delta t\,\Delta(\beta_2\mu^{n+1} - \beta_1\mu^{(2)}) \\
&= M\Delta t\,\Delta(\beta_2\mu^{n+1} + (\alpha_{22}-1)\beta_1\mu^{(2)} + (\alpha_{11}(\alpha_{22}-1) + \alpha_{21})\mu^{(1)}).
\end{aligned}$$

Then,

$$\begin{aligned}
&\mathcal{E}(\phi^{n+1}) - \mathcal{E}(\phi^n) \\
&\leq -M\Delta t\Big(\Big(\nabla\mu^{n+1}, \nabla(\beta_2\mu^{n+1} + (\alpha_{22}-1)\beta_1\mu^{(2)} + (\alpha_{11}(\alpha_{22}-1)+\alpha_{21})\mu^{(1)})\Big) \\
&\qquad + \Big(\nabla\mu^{(2)}, \nabla(\beta_1\mu^{(2)} - \alpha_{10}\mu^{(1)})\Big) + \Big(\nabla\mu^{(1)}, \nabla\mu^{(1)}\Big)\Big) \\
&= -M\Delta t \int_\Omega (\nabla\mu^{n+1}, \nabla\mu^{(2)}, \nabla\mu^{(1)})\,\mathbf{M}\,(\nabla\mu^{n+1}, \nabla\mu^{(2)}, \nabla\mu^{(1)})^T\,d\mathbf{x}.
\end{aligned}$$

Since $\mathbf{M}$ is positive semi-definite, $\mathcal{E}(\phi^{n+1}) - \mathcal{E}(\phi^n) \leq 0$. This completes the proof. □

Examples of the coefficients of the scheme (5), satisfying the stability condition (6), are

$$\alpha_{10} = \frac{1}{2}, \ \alpha_{11} = \frac{1}{2}, \quad \alpha_{20} = \frac{1}{2}, \ \alpha_{21} = \frac{3}{2}, \quad \alpha_{22} = -1, \ \beta_1 = 1, \ \beta_2 = 1, \tag{7}$$

$$\alpha_{10} = \frac{7}{6}, \ \alpha_{11} = -\frac{1}{6}, \ \alpha_{20} = \frac{7}{6}, \ \alpha_{21} = \frac{5}{6}, \quad \alpha_{22} = -1, \ \beta_1 = \frac{3}{2}, \ \beta_2 = \frac{3}{2}, \tag{8}$$

$$\alpha_{10} = \frac{7}{4}, \ \alpha_{11} = -\frac{3}{4}, \ \alpha_{20} = \frac{7}{4}, \ \alpha_{21} = \frac{1}{4}, \quad \alpha_{22} = -1, \ \beta_1 = 2, \ \beta_2 = 2, \tag{9}$$

$$\alpha_{10} = \frac{23}{10}, \ \alpha_{11} = -\frac{13}{10}, \ \alpha_{20} = \frac{23}{10}, \ \alpha_{21} = -\frac{3}{10}, \ \alpha_{22} = -1, \ \beta_1 = \frac{5}{2}, \ \beta_2 = \frac{5}{2}. \tag{10}$$

3. Numerical Experiments

3.1. Numerical Implementation

In order to make order of accuracy in space compatible with second-order in time, we employ the Fourier spectral method [21–23] in space for the scheme (5) to arrive at fully discrete second-order SSP-IMEX-RK method. Then, the fully discrete second-order SSP-IMEX-RK method with (6) can be proved similarly to preserve the energy dissipation law in the fully discrete level.

We consider a two-dimensional space $\Omega = [0, L_x] \times [0, L_y]$ for simplicity and clarity of exposition. One- and three-dimensional cases are defined analogously. Let N_x and N_y be positive integers and $\Delta x = L_x/N_x$ and $\Delta y = L_y/N_y$ be the space step sizes. In order to solve with the periodic boundary condition, we employ the discrete Fourier transform: for $k_x = 0, 1, \ldots, N_x - 1$ and $k_y = 0, 1, \ldots, N_y - 1$,

$$\widehat{\phi}_{k_x k_y} = \sum_{l_x=0}^{N_x-1} \sum_{l_y=0}^{N_y-1} \phi_{l_x l_y} e^{-i(x_{l_x}\xi_{k_x} + y_{l_y}\xi_{k_y})},$$

where $x_{l_x} = l_x \Delta x$, $\xi_{k_x} = 2\pi k_x/L_x$, $y_{l_y} = l_y \Delta y$, and $\xi_{k_y} = 2\pi k_y/L_y$. Then, the first-step of (5) can be rewritten in the form

$$\begin{aligned} &\phi^{(1)} - M\Delta t\, \mathcal{F}^{-1}\left[-(\xi_{k_x}^2 + \xi_{k_y}^2)\left(\mathcal{F}\left[(\phi^{(1)})^3\right] + \epsilon^2(\xi_{k_x}^2 + \xi_{k_y}^2)\mathcal{F}\left[\phi^{(1)}\right]\right)\right] \\ &= \phi^n + M\Delta t\, \mathcal{F}^{-1}\left[(\xi_{k_x}^2 + \xi_{k_y}^2)\mathcal{F}\left[\phi^n\right]\right], \end{aligned} \tag{11}$$

where $\mathcal{F}$ denotes the discrete Fourier transform and $\mathcal{F}^{-1}$ its inverse transform.

The nonlinearity in Equation (11) comes from $(\phi^{(1)})^3$ and this can be handled using the truncated Taylor expansion [21–23]

$$(\phi^{n,m+1})^3 \approx (\phi^{n,m})^3 + 3(\phi^{n,m})^2(\phi^{n,m+1} - \phi^{n,m})$$

for $m = 0, 1, \ldots$. We then develop a fixed point iteration method as

$$\begin{aligned} &\phi^{n,m+1} - M\Delta t\, \mathcal{F}^{-1}\left[-(\xi_{k_x}^2 + \xi_{k_y}^2)\left(\mathcal{F}\left[3(\phi^{n,m})^2\phi^{n,m+1}\right] + \epsilon^2(\xi_{k_x}^2 + \xi_{k_y}^2)\mathcal{F}\left[\phi^{n,m+1}\right]\right)\right] \\ &= \phi^n + M\Delta t\, \mathcal{F}^{-1}\left[(\xi_{k_x}^2 + \xi_{k_y}^2)\mathcal{F}\left[\phi^n + 2(\phi^{n,m})^3\right]\right], \end{aligned} \tag{12}$$

where $\phi^{n,0} = \phi^n$, and we set

$$\phi^{(1)} = \phi^{n,m+1}$$

if a relative l_2-norm of the consecutive error $\frac{\|\phi^{n,m+1} - \phi^{n,m}\|_2}{\|\phi^{n,m}\|_2}$ is less than a tolerance *tol*.

In this paper, the biconjugate gradient (BICG) method is used to solve the system (12), and we use the following preconditioner P to accelerate the convergence speed of the BICG algorithm:

$$P = I - M\Delta t\, \Delta \left(\bar{A} I - \epsilon^2 \Delta \right),$$

where $\bar{A}$ is the average value of $3(\phi^{n,m})^2$, i.e., $\bar{A} = \frac{1}{N_x N_y} \sum_{l_x=0}^{N_x-1} \sum_{l_y=0}^{N_y-1} 3(\phi^{n,m}_{l_x l_y})^2$. The stopping criterion for the BICG iteration is that the relative residual norm is less than tol.

The second- and third-steps of (5) are implemented analogously.

3.2. Convergence Test

We demonstrate the convergence of the proposed method with an initial condition [11]

$$\phi(x, y, 0) = 0.25 \sin(2\pi x) \cos(2\pi x).$$

The computational domain is $\Omega = [0, 1] \times [0, 1]$. We set $M = 10^{-3}$, $\epsilon = 10^{-2}$, and $tol = 10^{-7}\Delta t$, and compute $\phi(x, y, t)$ for $0 < t \leq T = 0.4$. The coefficients in (7) are used and the grid size is fixed to $\Delta x = \Delta y = 1/256$ which provides enough spatial accuracy. In order to estimate the convergence rate with respect to Δt, simulations are performed by varying $\Delta t = T/2, T/2^2, \ldots, T/2^6$. Figure 1 shows the relative l_2-errors of $\phi(x, y, T)$ for various time steps. Here, the error is computed by comparison with a reference numerical solution using $\Delta t = T/2^8$, i.e., is defined as $\frac{\|\phi^{\Delta t} - \phi^{\text{ref}}\|_2}{\|\phi^{\text{ref}}\|_2}$, where $\phi^{\Delta t}$ is a solution with a time step Δt and ϕ^{ref} is the reference solution. It is observed that the method is second-order accurate in time.

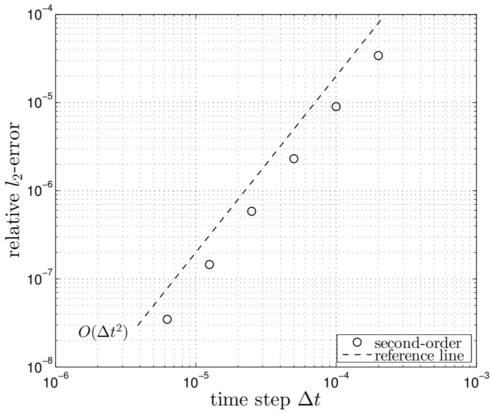

Figure 1. Relative l_2-errors of $\phi(x, y, T = 0.4)$ for $\Delta t = T/2, T/2^2, \ldots, T/2^6$ with $\epsilon = 10^{-2}$ and $\Delta x = \Delta y = 1/256$.

3.3. Energy Stability of the Proposed Method

In order to investigate the energy stability of the proposed method, we take an initial condition as

$$\phi(x, y, 0) = \text{rand}(x, y).$$

The computational domain is $\Omega = [0, 1] \times [0, 1]$. Here, $\text{rand}(x, y)$ is a random number between -0.01 and 0.01 at the grid points, and we use $M = 1$, $\epsilon = 10^{-2}$, $\Delta x = \Delta y = 1/256$, $tol = 10^{-5}\Delta t$, and coefficients in (7). Figure 2 shows the evolution of the energy and its difference with different time steps. All the energy curves are nonincreasing in time even for sufficiently large time steps. Figure 3 shows the evolution of $\phi(x, y, t)$ with $\Delta t = 2^{-9}$.

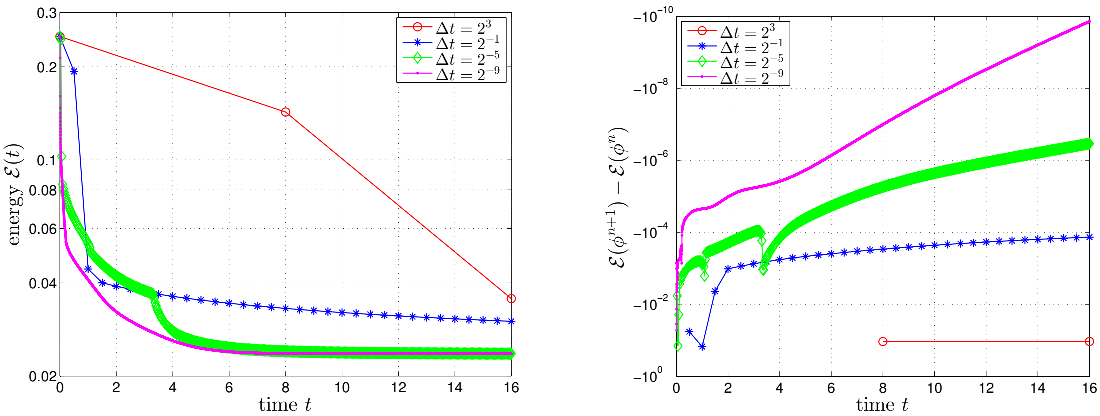

Figure 2. Evolution of the energy (**left**) and its difference (**right**) with different time steps.

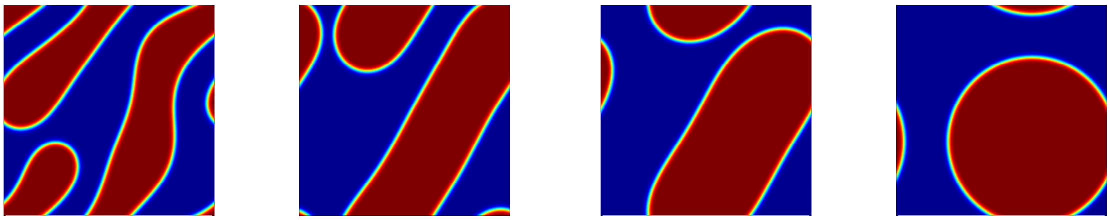

$t = 0.5$ $t = 2$ $t = 3.5$ $t = 16$

Figure 3. Evolution of $\phi(x, y, t)$ with $\epsilon = 10^{-2}$, $\Delta x = \Delta y = 1/256$, and $\Delta t = 2^{-9}$. In each snapshots, the red, green, and blue regions indicate $\phi = 1, 0$, and -1, respectively.

4. Conclusions

In this work, we investigated energy stability of the second-order (three-stage) SSP-IMEX-RK method for the CH equation with the polynomial double-well free energy density $F(\phi) = \frac{1}{4}(\phi^2 - 1)^2$. Under the stability condition, unconditional strong energy stability of the second-order method was proved theoretically. And, since the nonlinear convex splitting of $\mathcal{E}(\phi)$ was used compared to the linear convex splitting presented in [14], the restriction for the convexity of split energies was removed. We carried out numerical experiments to verify the accuracy and energy stability of the method.

We note that a choice of coefficients of the method may affect a convergence constant. An optimal choice of coefficients in terms of accuracy can be considered as the scope of future research. And we also note that there is a difficulty associated with the singularity as ϕ approaches -1 or 1 for a logarithmic free energy density $F(\phi) = \frac{\theta}{2}\left[(1+\phi)\ln\left(\frac{1+\phi}{2}\right) + (1-\phi)\ln\left(\frac{1-\phi}{2}\right)\right] + \frac{\theta_c}{2}(1-\phi^2)$. In order to avoid this, one can consider to apply a regularization to the logarithmic function [24,25] or develop a positivity-preserving scheme [26]. An extension of our method to the case of logarithmic free energy density using such approaches requires further investigation.

Funding: This work was supported by the National Research Foundation of Korea (NRF) grant funded by the Korea government (MSIT) (No. 2019R1C1C1011112).

Acknowledgments: The corresponding author thanks the reviewers for the constructive and helpful comments on the revision of this article.

Conflicts of Interest: The author declares no conflict of interest.

References

1. Cahn, J.W.; Hilliard, J.E. Free energy of a nonuniform system. I. Interfacial free energy. *J. Chem. Phys.* **1958**, *28*, 258–267. [CrossRef]
2. Chen, L.-Q. Phase-field models for microstructure evolution. *Annu. Rev. Mater. Res.* **2000**, *32*, 113–140. [CrossRef]

3. Gomez, H.; Hughes, T.J.R. Provably unconditionally stable, second-order time-accurate, mixed variational methods for phase-field models. *J. Comput. Phys.* **2011**, *230*, 5310–5327. [CrossRef]
4. Guan, Z.; Lowengrub, J.S.; Wang, C.; Wise, S.M. Second order convex splitting schemes for periodic nonlocal Cahn–Hilliard and Allen–Cahn equations. *J. Comput. Phys.* **2014**, *277*, 48–71. [CrossRef]
5. Elliott, C.M.; Stuart, A.M. The global dynamics of discrete semilinear parabolic equations. *SIAM J. Numer. Anal.* **1993**, *30*, 1622–1663. [CrossRef]
6. Eyre, D.J. Unconditionally gradient stable time marching the Cahn–Hilliard equation. *MRS Proc.* **1998**, *529*, 39–46. [CrossRef]
7. Du, Q.; Nicolaides, R.A. Numerical analysis of a continuum model of phase transition. *SIAM J. Numer. Anal.* **1991**, *28*, 1310–1322. [CrossRef]
8. Yang, X. Linear, first and second-order, unconditionally energy stable numerical schemes for the phase field model of homopolymer blends. *J. Comput. Phys.* **2016**, *327*, 294–316. [CrossRef]
9. Shin, J.; Lee, H.G.; Lee, J.-Y. Unconditionally stable methods for gradient flow using Convex Splitting Runge–Kutta scheme. *J. Comput. Phys.* **2017**, *347*, 367–381. [CrossRef]
10. Shen, J.; Xu, J.; Yang, J. The scalar auxiliary variable (SAV) approach for gradient flows. *J. Comput. Phys.* **2018**, *353*, 407–416. [CrossRef]
11. Gong, Y.; Zhao, J. Energy-stable Runge–Kutta schemes for gradient flow models using the energy quadratization approach. *Appl. Math. Lett.* **2019**, *94*, 224–231. [CrossRef]
12. Gong, Y.; Zhao, J.; Wang, Q. Arbitrarily high-order unconditionally energy stable SAV schemes for gradient flow models. *Comput. Phys. Commun.* **2019**, in press. [CrossRef]
13. Gong, Y.; Zhao, J.; Wang, Q. Arbitrarily high-order linear schemes for gradient flow models. *arXiv* **2019**, arXiv:1910.07211.
14. Song, H. Energy SSP-IMEX Runge–Kutta methods for the Cahn–Hilliard equation. *J. Comput. Appl. Math.* **2016**, *292*, 576–590. [CrossRef]
15. Ascher, U.M.; Ruuth, S.J.; Wetton, B.T.R. Implicit-explicit methods for time-dependent partial differential equations. *SIAM J. Numer. Anal.* **1995**, *32*, 797–823. [CrossRef]
16. Ascher, U.M.; Ruuth, S.J.; Spiteri, R.J. Implicit–explicit Runge–Kutta methods for time-dependent partial differential equations. *Appl. Numer. Math.* **1997**, *25*, 151–167. [CrossRef]
17. Shu, C.-W.; Osher, S. Efficient implementation of essentially non-oscillatory shock-capturing schemes. *J. Comput. Phys.* **1988**, *77*, 439–471. [CrossRef]
18. Gottlieb, S.; Shu, C.-W. Total variation diminishing Runge-Kutta schemes. *Math. Comp.* **1998**, *67*, 73–85. [CrossRef]
19. Gottlieb, S.; Shu, C.-W.; Tadmor, E. Strong stability-preserving high-order time discretization methods. *SIAM Rev.* **2001**, *43*, 89–112. [CrossRef]
20. Wang, C.; Wise, S.M. An energy stable and convergent finite-difference scheme for the modified phase field crystal equation. *SIAM J. Numer. Anal.* **2011**, *49*, 945–969. [CrossRef]
21. Shin, J.; Lee, H.G.; Lee, J.-Y. First and second order numerical methods based on a new convex splitting for phase-field crystal equation. *J. Comput. Phys.* **2016**, *327*, 519–542. [CrossRef]
22. Lee, H.G.; Shin, J.; Lee, J.-Y. First- and second-order energy stable methods for the modified phase field crystal equation. *Comput. Appl. Mech. Eng.* **2017**, *321*, 1–17. [CrossRef]
23. Lee, H.G. An energy stable method for the Swift–Hohenberg equation with quadratic–cubic nonlinearity. *Comput. Methods Appl. Mech. Eng.* **2019**, *343*, 40–51. [CrossRef]
24. Barrett, J.W.; Blowey, J.F. An error bound for the finite element approximation of the Cahn–Hilliard equation with logarithmic free energy. *Numer. Math.* **1995**, *72*, 1–20. [CrossRef]
25. Barrett, J.W.; Blowey, J.F. An error bound for the finite element approximation of a model for phase separation of a multi-component alloy. *IMA J. Numer. Anal.* **1996**, *16*, 257–287. [CrossRef]
26. Chen, W.; Wang, C.; Wang, X.; Wise, S.M. Positivity-preserving, energy stable numerical schemes for the Cahn-Hilliard equation with logarithmic potential. *J. Comput. X* **2019**, *3*, 100031.

© 2019 by the authors. Licensee MDPI, Basel, Switzerland. This article is an open access article distributed under the terms and conditions of the Creative Commons Attribution (CC BY) license (http://creativecommons.org/licenses/by/4.0/).